

An investigation into catalysts to improve the low temperature performance of an SCR

Youhong Xiao¹, Peilin Zhou¹, Wenping Zhang²

1. Department of Naval Architecture and Marine Engineering
Universities of Glasgow and Strathclyde, Scotland, UK

2. College of Power and Energy,
Harbin Engineering University, Heilongjiang P.R. China

Abstract

Selective catalytic reduction with NH_3 is considered as one of the most effective technologies controlling NO_x emission. Metal Fe based catalysts were used in the investigation to improve the low temperature performance of NO_x conversion. The temperature range studied was between 150 °C and 350 °C with the interval of 50 °C. The honeycomb catalysts were prepared by an impregnation method. The study also included characterization of catalysts by BET, XRD, H_2 -TPR, SEM and XPS methods.

It is found an increase in metal Fe content from 2 to 6 % wt. offers an improvement in the catalytic performance. However, a further increment in Fe content will result in a decrease in its performance. More than 90 % NO_x conversion rate could be achieved over the Fe-based honeycomb catalyst at a low temperature by doping with Ni and Zr metal with different weights. Among all the catalysts studied, the mixed metal catalyst of Fe-Ni-Zr is found the most potential one, not only because of its higher NO_x conversion rate at a low temperature, but also because of its wider operation temperature window. The effect of gas hourly space velocity (GHSV) was also investigated in the study and results show as GHSV increases that reduction of NO_x is decreased.

Keywords: NH_3 -SCR; ceramic honeycomb; Fe-based catalysts; low temperature

1 Introduction

There is worldwide interest in developing an efficient catalyst for the removal of NO_x from diesel engines exhaust systems. Diesel engines have been dominating the marine market for the provision of propulsion and electric power since 1970s. However, the emissions from marine diesel engines have seriously threatened the environment and are considered one of the major sources of air pollution. The total global NO_x emissions from ships have been estimated as 10.2 million tons NO_x per year for a consumption of 150 million tons of marine fuel[44]. The pollutants emitted from marine vessels have damaged the ecological environment systems such as ozone layer destruction, global warming and acid rain, etc. Reduction of pollutants from marine diesel engines in particular NO_x , is critical to human health, welfare and continued prosperity.

The selective catalytic reduction (SCR) of NO_x with NH_3 in the presence of excess oxygen has been proven at a commercial scale in the removal of NO_x from stationary sources [1, 2]. SCR catalysts used in industrial practice are based on TiO_2 , with vanadium oxide as the catalytic active phase. WO_3 and MoO_3 have been reported to be used as promoters [1, 3]. The range of operation temperature of these catalysts is between 300 °C and 400 °C.

For a large slow speed engine, the exhaust gas temperature is often below 300 °C after the turbocharger. Gas re-heating is required to ensure the efficiency of the catalytic conversion. In this sense, there has been a strong interest in developing SCR catalysts activating at a temperature lower than 300 °C. Some transition-metal-contained catalysts have been investigated to improve the low temperature performance of an SCR, such as chromic[4], $\text{NiSO}_4/\text{Al}_2\text{O}_3$ [5], $\text{MnOx}/\text{Al}_2\text{O}_3$ [6], V_2O_5 /carbon-coated

monoliths[7], iron–silica aerogels[8] and MnOx/NaY[9]. The use of these catalysts has shown an improvement of SCR activity to certain degree at a temperature below 200 °C under different condition. Iron catalysts have been extensively used in several processes related to NOx elimination, mainly due to its low cost compared with that of noble metals and its good performance of these catalysts with different reducing agents. It has been reported that Fe₂O₃ [10, 11, 12, 13, 14, 15, 16], Fe containing oxides [17, 18, 19, 20] and Fe-exchanged materials [21, 22, 23, 24, 25] have greater SCR activity than other types of catalyst. The process of selective catalytic reduction of NOx at a low temperature with ammonia has been investigated with metal Ni [26, 27, 28, 29], the results show that Ni is efficient for the reduction of NOx. ZrO₂ has better thermal stability and sulphur resistance[30], can be of a very high activity for NO reduction[31] [32] as a support. ZrO₂ is seldom used as the catalyst for an SCR, but reports [33, 34] have shown that a Zr catalyst is durable and highly active for NO reduction.

In the operation of the fixed-bed, a large volume of pellets or granules may cause high flow resistance and plugging problem due to particulates in flue gas. In contrast, honeycomb catalysts show low-pressure drop, high surface area, superior attrition resistance and low tendency to fly ash plugging [45, 46, 47]. For these reasons, the honeycomb vanadia–titania catalyst has been used in industry to remove NO from flue gas [48]. Based on the successful application of ceramic honeycomb, the paper presents a study on using a ceramic honeycomb structured catalyst. Fe, Fe-Ni, Fe-Ni-Zr catalysts are used to improve the low temperature conversion rate of NOx

2 Experiment

2.1 Catalyst preparation

In the study, a ceramic honeycomb substrate was cut into small columns, with 40 mm in length and 8 mm in diameter for laboratory test. After pre-treatment with nitric acid solution at 40%, the chosen nitrates were coated to the ceramic honeycomb substrates by an impregnation method. It is reported that the acid treatment of the substrate exhibits an increased surface area and improved dispersion of active components[36]. The catalysts, e.g. substrates coated with metal oxides were tested and analysed, including characterisation examination of the mixed oxides catalysts using XRD, TPR-H₂, XPS and SEM methods. These analyses allow to get the insight of the influence of meso-porosity on the performance of the catalysts prepared.

In this study, three types of catalyst, i.e. Fe and mixtures of Fe-Ni, and Fe-Ni-Zr are studied. The catalysts Fe, Ni and Zr were obtained from the mixture of the compounds of Fe(NO₃)₃, Ni(NO₃)₂ and Zr(NO₃)₄ solutions. Firstly the ceramic honeycomb substrate was impregnated in a heavy nitric acid solution at a mass concentration of 40 % for about 8 hours to clean its surface, then the substrate was washed to pH = 7 by distilled water. The treated honeycomb substrate was then dried at 150 °C for 8 hours before it was impregnated into the aqueous solution of nitrates for a day. Then, the substrate saturated by catalyst was dried at 250 °C for 8 hours and calcined in the air at 600 °C for 8 hours.

2.2 Characterisation of catalysts

A chemical catalytic process varies with the structures and constitutions of the catalyst. At a given structure, a catalyst is active in a chemical reaction, however, its reaction may not be active when it is at a different structure even the chemical compound of the catalyst remains unchanged. Therefore, it is important to measure the structures and constitutions of the catalysts.

BET surface area and pore diameter

The measurement of Brunauer-Emmett-Teller (BET) surface value (surface area per unit mass) and the pore diameter was conducted by N₂ adsorption. The instrument used is model ASAP2010, measuring the isothermal lines at -196 °C. From the principles of physisorption measurement with nitrogen, the BET surface area of catalysts was calculated by using the method discussed in reference^[37] in a combination with use of the data obtained from the isothermal lines at a pressure ranged from 0.1-1.0 bar. The measured data of the BET surface are shown in Table 1.

XRD characterisation

X-Ray Diffraction (XRD) is an effective method in identifying structures and constitutes of a catalyst where the measured data is compared with a standard XRD spectrum. An XRD meter, model: Y-500 was used in the experiment of this study. Cu-K α radiation ($\lambda = 1.54178 \text{ \AA}$) was used. Samples of the catalysts were loaded on a sample holder of a depth of 1 mm for the XRD scanning. The X-ray tube was operated at 30 kV and 20 mA with the diffraction angle set from 5° to 80°. The scanning speed applied in this analysis was 8 degree/min.

TPR measurement

Temperature programmed reduction (TPR) by H₂ was performed to study the activities of catalysts at different temperatures and concentrations.

A sample of 0.1 g of each catalyst (mixture) was loaded into the reactor and pretreated from 20 °C in an Ar gas stream (30 l/min) with a heating rate that increases the temperature of the sample at 8 °C per min upto 500 °C. Then the sample was kept at 500 °C for 30 min, followed by a cooling process with dry ice to 30 °C in the Ar gas. The pretreated sample was then exposed to a reductive gas mixture containing 5.4 % by vol. of H₂ in Ar at a flow rate of 30 l/min and with a heating rate of 10 °C/min from 30 °C to 900 °C. The consumption rate of H₂ was continually monitored using a chromatography thermal conductivity detector (TCD). It can be assumed that if a catalyst has a high H₂ consumption at a given range of temperature, the catalyst contains a high concentration of active components, implying its NO conversion rate is high at that temperature range.

XPS experiment

X-ray photoelectron spectroscopy (XPS) was used to study the chemical composition of the surface of catalysts. The multiphase catalytic reaction performs on the surface of solid, thus, the characteristics of the surface is determined by the concentration of active constitution of a catalytic. The characterisation of a catalyst includes structures, constitutions, distribution of activation, inter-action and inter-reaction among the active components.

In this study, XPS experiment was performed at a room temperature by a spectrum analyser, model PHI-5700. The measurement was carried out under an ultra-high vacuum condition (5×10^{-6} kPa). An aluminium-based K α monochromatic X-ray (1486.6 eV), emitting impact energy at 20 eV, was used. Data acquisition was carried out with a measurement step of 0.8 eV. The binding energy was determined with use of a reference value taken from the C1s line given by the instrument manufacturer at 284.62 eV. The energy analyser was set with a fixed impact of energy at 20 eV.

Scanning electron microscopy (SEM) experiment

The surface morphology of the samples was investigated using a JSM-6480 SEM analyzer with a tungsten filament and an accelerating voltage of 15 kV equipped with a CCD camera. Before the scanning, the samples were crushed to powder and the powder samples were spread onto a double-

sided carbon tape, and coated with gold (20–30 nm thickness) in order to increase the conductivity and therefore the quality of the measurement results.

2.3 Catalytic activity tests

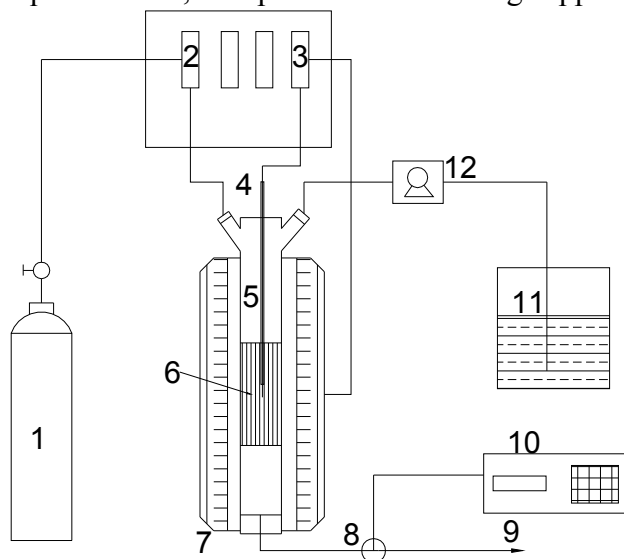
The honeycomb substrates coated with different metallic oxides as shown in Table 1 for laboratory scale experiment were tested in a selective reduction reactor under a condition close to an isothermal axial profile at every reaction temperature. The support catalysts are presented by Fe(a)Ni(b)Zr(c), where (a), (b) and (c) represent the weight percent of Fe, Ni and Zr in the catalysts including the weight of the substrate.

Table 1 BET surface and mass percentage of investigated catalysts

Catalyst	BET (m ² /g)
Fe(4)Ni(0)Zr(0)	131.0
Fe(6)Ni(0)Zr(0)	134.6
Fe(8)Ni(0)Zr(0)	114.1
Fe(6)Ni(1)Zr(0)	185.3
Fe(6)Ni(2)Zr(0)	246.2
Fe(6)Ni(2)Zr(1)	256.2
Fe(6)Ni(2)Zr(2)	252.4

2.4 Description of test rig

As shown in Figure 1 and 2, urea solution is used to provide gas phase ammonia which is employed by most SCR systems as the reducing agent. The ammonia generated from urea is in either anhydrous or aqueous form, is vaporized before being supplied to the reactor (SCR).



1. Sample gas
2. Mass flow controller
3. Temperature controller
4. Thermocouple

5. Reactor
 6. Honeycomb catalyst substrate
 7. Electric furnace
 8. 3 way valve
 9. Vent
 10. NO_x and O₂ analyser
 11. Urea solution tank
 12. Urea mass flow control pump
- Figure 1 Schematic diagram of testing rig

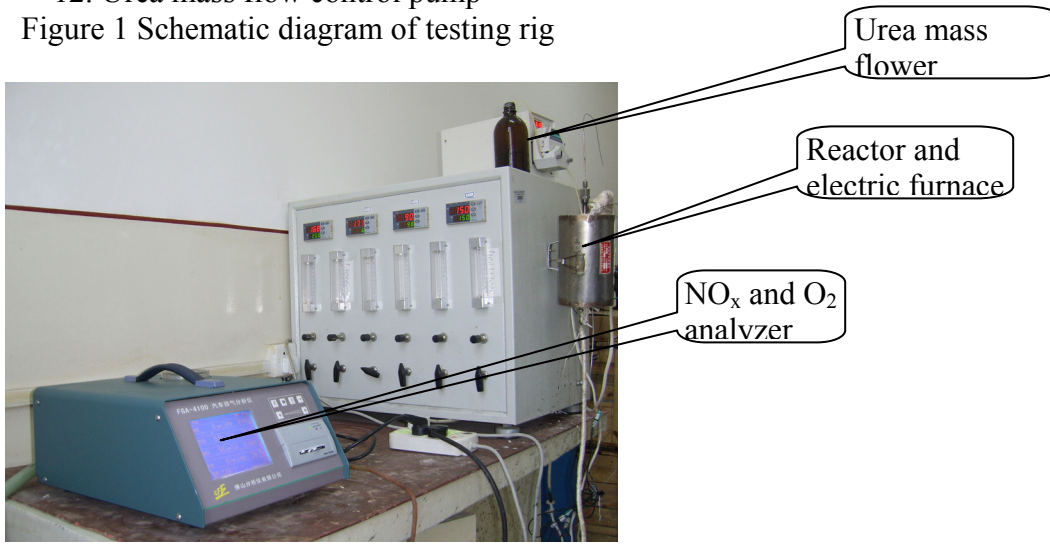
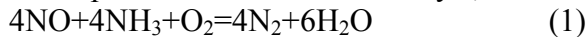


Figure 2 SCR testing equipment

In the presence of a suitable catalyst, the following processes will take place inside the reactor:



NO_x in diesel exhaust gases usually consists of over 95% of NO and less than 5% of NO₂. Therefore, the main reaction of an SCR with ammonia is represented by equation (1).

Equation 1 indicates that one mole of NH₃ is required to remove one mole of NO. The presence of a catalyst lowers the required activation energy for the reduction and increases the NO conversion rate.

A lab-scale fixed-bed reactor (stainless steel) with an inter diameter of 10 mm and length of 200 mm was used in the experiment to investigate the activity of each chosen synthetic catalyst in reactor with NH₃ at the atmosphere pressure. A catalyst substrate of 8 mm in diameter and 40 mm in length was installed inside the reactor for the catalytic testing, as shown in Figure 1. The reaction temperature was controlled by a programmed temperature controller from 150 °C to 350 °C with an increment of 50 °C. Every measurement temperature was maintained for 30 min before sampling measurement was taken.

The sample gas was prepared to simulate an engine exhaust gas, comprising 1200 ppm NO, and 2 % by vol. of O₂ balanced by N₂, was fed into the reactor with a flow rate of 180 ml/min controlled by a flow meter. 10% by mass of urea solution was used to provide the required NH₃. The urea solution was injected to the reactor at a flow rate of 0.015 ml/min. It vaporises inside the reactor due to heating and releases NH₃ to perform the chemical reactions presented in equation 1 and 2.

A gas analyser, model-FGA-4100, was used to measure the concentration of NO and O₂ before and after the reactor. The reaction results were evaluated in terms of NO conversion rate, i.e. the ratio of NO converted via the reactor to the total NO level before the reactor.

3 Results and discussion

3.1 SCR performance with different catalysts

3.1.1 Effect of Fe catalyst

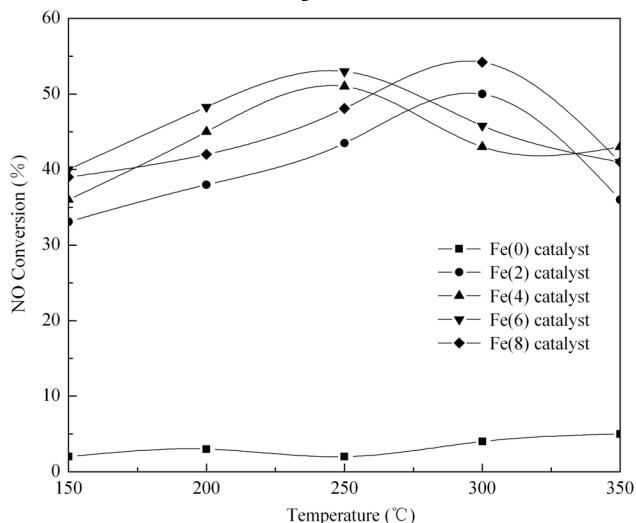


Figure 3 Catalytic performance with Fe catalyst

Figure 3 shows the results of NO conversion rate with Fe as the catalyst. The reaction temperature was from 150 to 350 °C. Other test conditions were GHSV= 12000 h⁻¹, NO = NH₃ =1200 ppm, 2.0 vol. % O₂, N₂ balance.

The balance between dispersion and loading of metal catalysts is a vital factor, which affects the catalytic activity directly. Increasing the catalyst loading will result in an aggregation of the catalyst and a decrease in the dispersion. Although low loading is beneficial for a good dispersion, it results in a low number of the active sites over the support, hence, the catalytic performance will be reduced. NO conversion rates with different Fe loadings are shown in Figure 3. It can be found that at 250°C the NOx conversion rate increases as the Fe loading increases and reaches to its maximum at 53% when loading is 6%wt. . When Fe content is 8 %wt. , the NO conversion rate is reduced to 43 %. Possible reason for the drop of NOx conversion rate at a high loading is there might be a clustering of Fe species when its loading is high. This is in consistence with the results shown in Table 1, where the BET surface at 8 %wt. of Fe catalyst is significantly small compared with that at 6 %wt.. Therefore, the catalysts with 6 %wt. Fe content were selected for the subsequent experimental work. Figure 3 also shows that the low temperature performance of the catalytic reduction is improved significantly.

3.1.2 Effect of Fe dopped with Ni and Zr

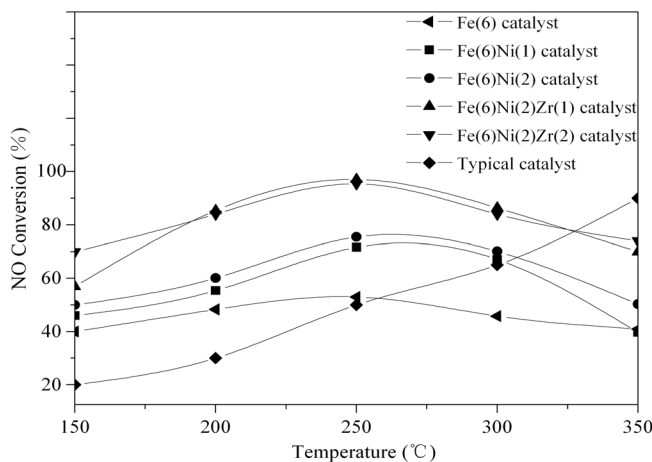


Figure 4 NO_x reduction rate with different mixtures of catalysts

Figure 4 presents NO conversion rate with different mixtures of catalysts as a function of reaction temperature varying from 150 to 350 °C. Other test conditions were GHSV = 12000 h⁻¹, NO = NH₃ = 1200 ppm, 2.0 vol% O₂, N₂ balance.

Based on the catalytic results of different Fe loading catalysts, different loadings of metal Ni and Zr were doped into the 6 %wt Fe catalyst. As shown in figure 4, the combination of iron-nickel-cerium (Fe-Ni-Zr) offers the highest reaction activity among the catalysts studied at the full temperature measurement range, with the maximum NO conversion rate of 95.1 % at a temperature around 250°C. The activity of Fe itself is the lowest, reaching its maximum NO conversion rate of 52% at 250 °C. It is observed that the order of activeness of the catalysts for NO conversion is Fe(6)Ni(2)Zr(2)>Fe(6)Ni(2)Zr(1)>Fe(6)Ni(2)> Fe(6)Ni(1)>Fe(6).

The activity of Fe catalyst was substantially lower than that of other Fe based oxides catalysts, Thus, iron alone could hardly be used in the application due to its low activity. The catalysts iron-nickel (Fe-Ni) have an improved activity than Fe itself and the NO conversion increased more rapidly when the temperature was over 200 °C, but then dropped again when the temperature was over 300 °C. However, the activity of Fe-Ni catalyst is lower than 50% when the temperature is higher than 300 °C. The Fe-Ni catalyst with 2 %wt Ni has a little increasing catalytic performance than the Fe-Ni catalyst with 1 %wt Ni. It seems that the effect of increasing Ni on the NO conversion is not obvious. Based on this, the metal Zr was introduced to promote the NO conversion rate.

After the introduction of Zr, it was found that the Fe-Ni-Zr catalyst has a superior activity during the whole temperature window, especially in the lower temperature range. But the NO conversion of the catalysts dropped slightly when the temperature was over 300 °C.

For the purpose of comparison, a current commonly used commercial catalyst (V₂O₅/WO₃)[38] in an SCR system is also presented in Figure 4, where it exhibits a high conversion rate in a temperature above 300 °C, whereas, its low NO conversion rate is poor. According to the catalytic results of Fe(6)Ni(2)Zr(2) catalyst, the catalyst can enhance the NO conversion dramatically at a low temperature.

3.1.3 Effect of Gas hourly space velocity (GHSV) on NO conversion

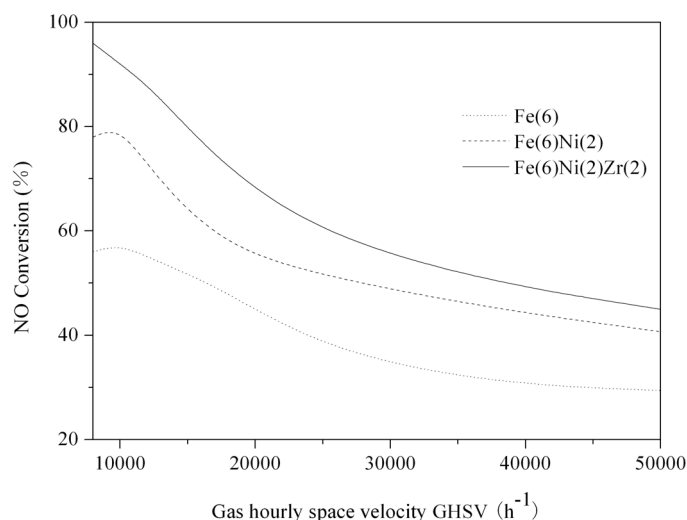


Figure 5. NO reduction rate change with GHSV

Figure 5 shows catalytic performance of 6 %wt Fe catalyst doped with Ni and Zr as a function of GHSV at a temperature of 250 °C. Other test conditions were NO = NH₃ =1200 ppm, 2.0 vol% O₂, N₂ balance.

Space velocity is defined as the volume ratio of gas flow rate relative to the catalyst volume flow rate, expressed in per-hour (why?). At a constant gas flow rate, space velocity is inversely proportional to catalyst volume such that decreasing catalyst volume corresponds to increasing space velocity. Typically, an increase in the space velocity decreases the NO conversion for most catalysts since the net residence time of the gas species over the surface of the catalyst decreases. To some extent, temperature plays a role in determining the degree to which space velocity affects the NO conversion[39].

According to the above results, the temperature of best catalytic performance of the investigated catalysts is at 250 °C. Thus the temperature was selected to investigate the effort of GHSV on NO conversion.

Figure 5 shows the effect of space velocity on the conversion rate of NO. The NO_x conversion rate is high when the space velocity is low. This is because a low space velocity properly is beneficial for the diffusion, adsorption and reaction of the reactants and it also promote the desorption and diffusion of reaction products. When the space velocity is high, the contacting time of reactants and catalysts becomes less which will lead to that the contacting time of the reactants and the catalyst is not enough for the catalytic reaction, thus, the NO conversion rate drops quickly. Therefore it is beneficial to decrease the space velocity for the NO conversion, however, to achieve a low space velocity for a given engine exhaust system, the size (cross section area or length) of the catalyst converter will have to be increased accordingly.

3.2 X-Ray Diffraction

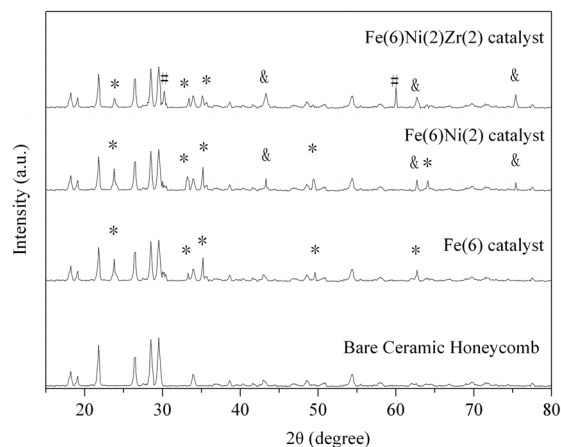


Figure 6 XRD patterns of bare ceramic honeycomb, Fe(6) catalyst, Fe(6)Ni(2) catalyst and Fe(6)Ni(2)Zr(2) catalyst. (*: Fe₂O₃; &: NiO; #:ZrO₂)

Figure 6 shows the XRD patterns of the pure honeycomb ceramic and that supported with Fe₂O₃, NiO, ZrO or a mixture of different oxides. All the samples exhibited the typical peaks of the ceramic honeycomb, indicating that the structure of the ceramic honeycomb remained intact after the treatment. Compare to the intensity of the XRD peaks of the bare ceramic honeycomb, the intensity of the peaks of the catalysts under investigation decreased. The reason for this is that the addition of metals causes the dispersion of the elements on the ceramic honeycomb.

As shown in Fig 6, typical lines of Fe catalyst were detected at 23.8°, 33.3°, 35.2°, 49.5° and 64.2°(2θ). These lines were due to the strongest lines of Fe₂O₃.

The additional lines appear in the XRD pattern of Fe-Ni catalyst at 43.3, 43.5, and 62.7°(2θ). These lines detected to be NiO. And the typical lines of Ni₂O₃ did not find. In the catalysts of Fe-Ni catalysts, the diffraction peaks of Fe₂O₃ were observed the same phrase as Fe catalyst,

The diffractions at 30.2° and 60° (2θ) due to zirconia phase [33] [35] were clearly observed on the Fe-Ni-Zr catalyst sample. It is found that some of the lines of Fe disappeared and the intensity of some Fe₂O₃ decrease. This suggested that the Zr doping caused the dispersion of Fe and they interacted strongly.

3.3 Temperature programme reduction over Fe-based catalysts

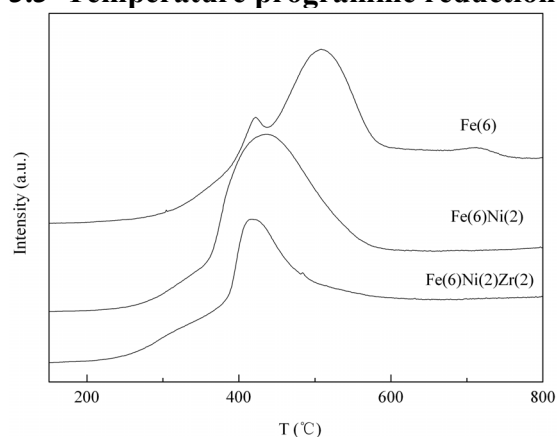


Figure 7 TPR profiles of Fe(6), Fe(6)Ni(2) and Fe(6)Ni(2)Zr(2) catalyst

Temperature programmed reduction (TPR) was used to characterize the ceramic honeycomb supported catalysts as shown in Figure 7. During the process of temperature programmed reduction, the reduction sequence of iron oxide is as following $\text{Fe}_2\text{O}_3 \rightarrow \text{Fe}_3\text{O}_4 \rightarrow \text{FeO} \rightarrow \text{Fe}$.

From various H_2 -TPR studies of Fe catalyst [40, 41, 42], there is general agreement that the peak for hydrogen consumption centered around 410 °C can be attributed to the reduction of the Fe_2O_3 to Fe_3O_4 in Fe species. The second reduction peak was assigned to the reduction of Fe_3O_4 to Fe^0 . But according to [31], there have two reduction peaks attributed to the reduction of Fe_3O_4 small nanoclusters to FeO , and then of FeO to Fe^0 . Some people thought that the two processes of the reduction from Fe_3O_4 into Fe and from FeO into Fe^0 is completed by one step, so the two reduction peaks should be one. Therefore there is only one reduction peak of hydrogen consumption

It is found that there is only one main peak of the Fe-Ni and Fe-Ni-Zr catalyst. The reason is that the doping of Ni and Zr changed the structure of pure iron catalyst, and the Ni, Zr interact with Fe and substrate strongly. Therefore there is no Ni and Zr reduction peak, and only has the reduction peak of the Fe_2O_3 to Fe_3O_4 . Meanwhile the peak moved to the lower temperature, and this leads to the decreasing of reduction reaction energy and make the reduction reaction much easier than the iron catalyst and cause it easier for the catalytic reaction.

3.4 X-ray photoelectron spectroscopy

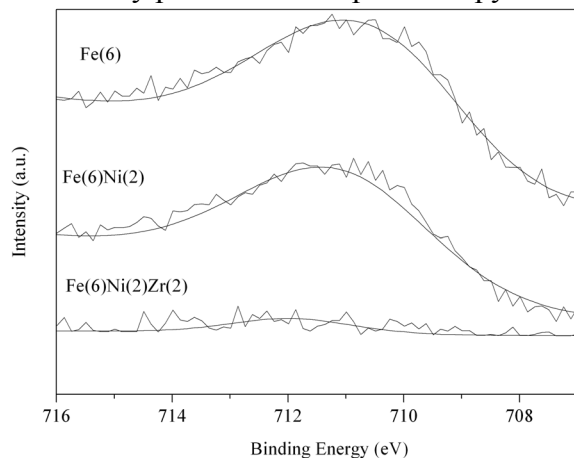


Figure 8 XPS spectra of Fe $2p_{3/2}$ on Fe(6), Fe(6)Ni(2) and Fe(6)Ni(2)Zr(2) catalyst

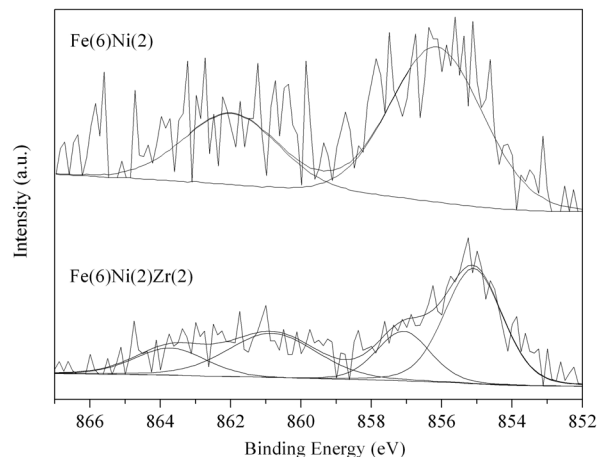


Figure 9 XPS spectra of Ni $2p$ on Fe(6)Ni(2) and Fe(6)Ni(2)Zr(2) catalyst

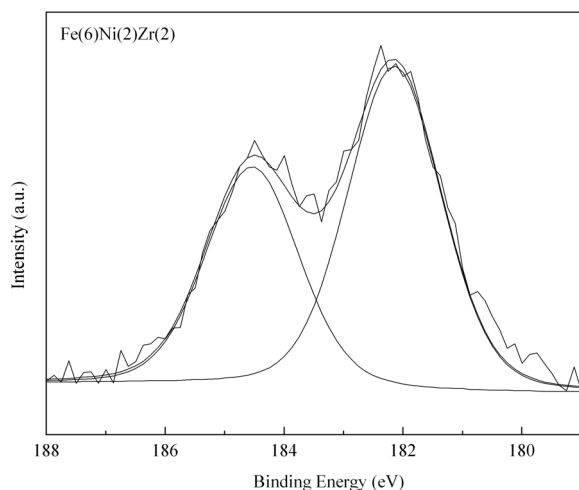


Figure 10 XPS spectrum of Zr 3d on Fe(6)Ni(2)Zr(2) catalyst

Figure 8 shows the XPS spectrum of Fe $2p_{3/2}$ on the Fe, Fe-Ni and Fe-Ni-Zr catalyst. A broad XPS band centered at 711.7 eV was observed on the sample of Fe catalyst. This value is close to the binding energy of $2p_{3/2}$ of iron in Fe_2O_3 [2, 3], indicating that iron in the Fe catalyst was mainly present as a valence of +3. After Ni was added, the peak was changed and the peak of Fe 2p had been broadened. As a general rule, if the formation of an interfacial oxide takes place, some modifications of the X-ray photoemission spectrum are expected to have an energy shift and/or the presence of satellite peaks[1]. It can be seen from Figure 8, the binding energy value was increased from 711.3 eV to 711.5 eV with the addition of Ni. With the further addition of Zr, the binding energy value was increased to 712 eV and the intensity of the peak values for this oxidation state was decreased dramatically.

Figure 9 illustrates Ni 2p XPS spectrum on both Fe-Ni and Fe-Ni-Zr catalyst. The presence of peak values at 856.0 and 862.5 eV of Fe-Ni catalyst is due to the binding energy of Ni $2p_{3/2}$ and Ni $2p_{1/2}$, respectively, since the nickel is in oxidation state +2. For catalyst of Fe-Ni-Zr, the peaks at 856.8 and 863.8 eV are attributed to the binding energies of $Ni^{2+} 2p_{3/2}$ and $Ni^{2+} 2p_{1/2}$, respectively. However, with the addition of Zr, the maximum intensity is decreased. Furthermore, there were two peaks, each appeared on the higher binding energy side of $Ni^{2+} 2p_{3/2}$ and $Ni^{2+} 2p_{1/2}$, respectively. Although the exact phase of these peaks were unknown, it is possible to consider that they were the mixture of iron oxides and nickel or zirconium oxides. Therefore, it was reasonable to conclude that in the catalyst of Fe-Ni-Zr, part of nickel, zirconium had interacted with iron and formed solid solution on the interface of these metals It can be seen from the SEM photos (Figure 11) of Fe-Ni-Zr catalyst.

Figure 10 shows the binding energy of the Zr 3d photoelectron reaches to its peaks at 182.3 and 184.5eV for Zr $3d_{5/2}$ and Zr $3d_{3/2}$ elements, respectively, due to existence of Zr^{+4} in the catalyst. The result is in consistent with the results of XRD.

3.5 Scanning electron microscopy

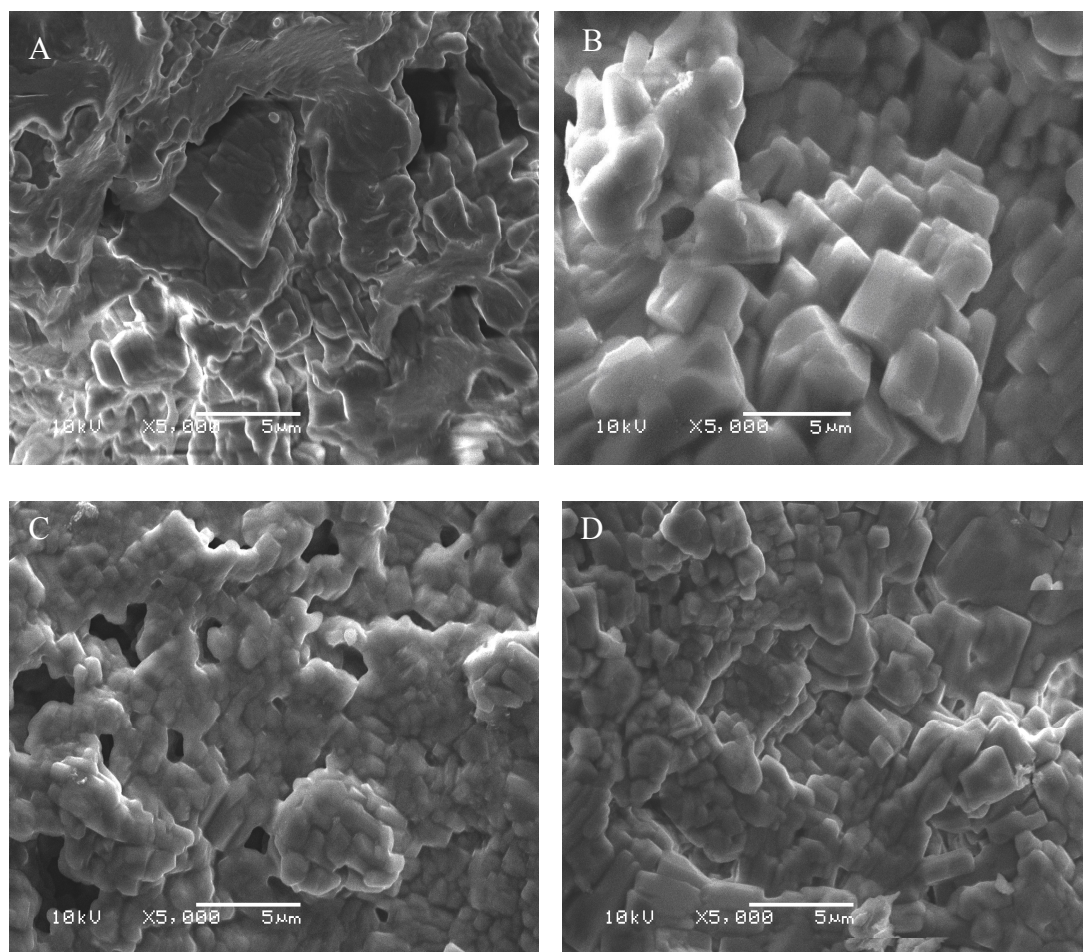


Figure 11 SEM photos of catalyst elements

Where: (A) bare ceramic honeycomb, (B) Fe(6) catalyst, (C) Fe(6)Ni(2) catalyst, (D) Fe(6)Ni(2)Zr(2) catalyst

The results of scanning electron microscopy (SEM) of bare honeycomb ceramic and after impregnation with iron, iron-nickel and iron-nickel-zirconium are shown in Figure 9 respectively.

As shown in Figure 9(A), the overall surface of bare ceramic was uneven, but the surface itself was smooth and there were many micropores on it, which would encourage the metal oxides to be dispersed evenly. After impregnated with the metal of iron, it can be seen that there are many small particle materials on the surface of catalyst as shown in Figure 9(B). The dispersion of the active location was presented in the form of particles and the catalyst disperses unevenly. Maybe this is the reason that the pure Fe catalyst has a low NO conversion. And it needs to be modified by doping other metal to improve its structure and enhance the catalytic performance. It was found from the Figure 9(C) that the surface of Fe(6)Ni(2) catalysts is smoother than Fe catalyst, otherwise there are also few micropores on the surface of Fe(6)Ni(2) catalysts, this is due to the doping of Ni metal not filling the vacancy of the Fe catalyst. This implies that doping the metal Ni can improve the activity of Fe catalyst in a certain extent, and need to be modified furthermore.

It can be seen from Figure 9(D) that iron, nickel and zirconium oxides on the catalyst are distributed more homogeneously and forms particles with smaller average diameter. Compared to Figure 9(C), the micropores of Fe(6)Ni(2) catalyst disappear and the interaction of these metals can be seen from the surfaces. The result is coincidental with that of TPR. Better dispersion of Fe(6)Ni(2)Zr(2) catalyst could account for the higher catalytic activity of the catalyst.

4 Conclusions

The paper has presented the results of an investigation into the NO_x conversion rate of Fe-based catalysts at a low temperature range, using ceramic honeycomb as the substrate. The study has revealed properties and their association with the NO_x reduction rate of the catalysts.

Conclusions have been reached that compared with the current commonly used catalysts, Fe-based catalysts have a much higher conversion rate of NO_x in an SCR under the temperature range of 150°C to 350°C. Results have shown that amongst the catalysts studied, the catalyst of combined Fe-Ni-Zr is the most active one for the SCR of NO by NH₃. Fe₂O₃ is the main active specie in the catalyst, while the addition of NiO and ZrO₂ is important to improve activities of the catalysts. Tests have found that the catalysts offer the highest NO_x reduction rate when the loading ratio of the catalysts is 6% wt. of Fe, 2% wt. of Ni and 2% wt. of Zr.

References

- [1] S. M. Cho, Properly Apply Selective Catalytic Reduction for NO_x Removal, Chemical Engineering Progress, January 1994, pp. 39–45
- [2] H. Bosch, F.J.I.G. Janssen, Lithium-Vanadium bronzes as model catalysts for the selective reduction of nitric oxide, Catalysis Today, Volume 4, Issue 2, January 1989, 139-154
- [3] M. F. H. Van Tol, M. A. Quinlan, F. Luck, G. A. Somorjai and B. E. Nieuwenhuys, The catalytic reduction of nitric oxide by ammonia over a clean and vanadium oxide-coated platinum foil, J. Catal. 129 (1991) 186
- [4] H. Schneider, U. Scharf, A. Wokaun, A. Baiker, Conjugated Polymer-Supported Catalysts - Polyaniline Protonated with 12-Tungstophosphoric Acid” Journal of Catalysis, Vol. 147, 1994, 545-551.
- [5] J.P. Chen, R.T. Yang, M.A. Buzanowski, J.E. Cichanowicz, Ind. Eng. Chem. Res. 29 (1990) 1431.
- [6] L. Singoredjo, R. Korver, F. Kapteijn, J. Moulijn, Appl. Catal. B 1 (1992) 297.
- [7] Z.P. Zhu, Z.Y. Liu, H.X. Niu, S.J. Liu, J. Catal. 187 (1999) 245.
- [8] P. Fabrizioli, T. Burgi, A. Baiker, “Environmental Catalysis on Iron Oxide–Silica Aerogels: Selective Oxidation of NH₃ and Reduction of NO by NH₃” Journal of Catalysis, Vol. 206, 2002, 143-154.
- [9] M. Richter, A. Trunschke, U. Bentrup, K.-W. Brzezinka, E. Schreier, M. Schneider, M.-M. Pohl, R. Fricke, “Selective Catalytic Reduction of Nitric Oxide by Ammonia over Egg-Shell MnO_x/NaY Composite Catalysts” Journal of Catalysis, Vol. 206, 2002, 98-113.
- [10] W. Weisweiler, B. Retzlaff and B. Hochstein, Staub-Reinhalt. Luft 3 (1988), p. 119.
- [11] G. Ramis, L. Yi, M. Turco, E. Kotur and R.J. Willey, J. Catal. 157 (1995), p. 523.
- [12] W. Weisweiler, E. Mallonn and O. Görke, Chem. Ing. Tech. 1–2 (2003), p. 72. Full Text via
- [13] L. Chmielarz, P. Kustrowski, M. Zbroja, W. Lasocha and R. Dziembaj, Catal. Today 90 (2004), p. 43.
- [14] W. Weisweiler and B. Maurer In: W. Essers, Editor, Dieselmotorentechnik 1998,
- [15] H. Bosch and F. Janssen, Catal. Today 2 (1988), p. 369.
- [16] A. Kato, S. Matsuda, F. Nakajima, M. Imanari and Y. Watanabe, J. Phys. Chem. 85 (1981), p. 1710.
- [17] A. Palmqvist, E. Jobson, L. Andersson, R. Granbro, M. Wendin, L. Megas, P. Nisius, A. Wiartalla, G. Lepperhoff, P. Blakeman, T. Ilkenhans, D. Webster, G. Haeffler, P. Voorde, P. Schmidt-Zhang, U. Guth, M. Wallin, SAE Paper 2004-01-1294.
- [18] S. Wu and K. Nobe, Ind. Eng. Chem. Prod. Res. Dev. 16 (1977), p. 136. Full Text via CrossRef
- [19] R.J. Willey, H. Lai and J.B. Peri, J. Catal. 130 (1988), p. 319.

- [20] R.J. Willey, E. Kotur, J. Kehoe, G. Busca, in: Y.A. Attia (Ed.), Proc. Int. Symp. Adv. Sol-Gel Process. Appl., 1994, p. 351.
- [21] R.Q. Long and R.T. Yang, *J. Catal.* 186 (1999), p. 254.
- [22] R.Q. Long and R.T. Yang, *Appl. Catal. B* 27 (2000), p. 87
- [23] R.Q. Long and R.T. Yang, *Appl. Catal. B* 33 (2001), p. 97.
- [24] R.Q. Long and R.T. Yang, *J. Catal.* 207 (2002), p. 274.
- [25] G. Qi, R.T. Yang and R. Chang, *Catal. Lett.* 87 (2003), p. 67.
- [26] B.I. Mosqueda-Jiménez, A. Jentys, K.Seshan, J.A.Lercher, Structure-activity relations for Ni-containing zeolites during NO reduction I. Influence of acid sites, *Journal of Catalysis* 218 (2003) 348
- [27] K.I. Shimizu, H. Maeshima, A. Satsuma, T. Hattori: *Appl. Catal. B*, 18, 163 (1998).
- [28] E.A. Efthimiadis, G. D. Lionta, S. C. Christoforou, I.A. Vasalos: *Catal. Today*, 40, 15 (1998).
- [29] Shujuan Zhang, Landong Li, Bin Xue, Jixin Chen, Naijia Guan, and Fuxiang Zhang, *React. Kinet. Catal. Lett. Vol. 89, No. 1*, 81–87 (2006)
- [30] N. Hickey, P. Fornasiero, J. Kašpar, M. Graziani, G. Martra, S. Coluccia, S. Biella, L. Prati and M. Rossi, *J. Catal.* 209 (2002), p. 271
- [31] R. Di Monte, P. Fornasiero, J. Kašpar, P. Rumori, G. Gubitosa and M. Graziani, *Appl. Catal. B* 24 (2000), p. 157.
- [32] N.A. Saidina Amin, C.M. Chong, SCR of NO with C₃H₆ in the presence of excess O₂ over Cu/Ag/CeO₂-ZrO₂ catalyst, *Chemical Engineering Journal* 113 (2005) 13–25
- [33] Chong Wang, Xiping Wang, Na Xing, Qing Yu, Yijing Wang *Applied, Catalysis A: General* 334 (2008) 137–146
- [34] Zhenping Zhu, Zhenyu Liu, Shoujun Liu, Hongxian Niu, Catalytic NO reduction with ammonia at low temperatures on V₂O₅/AC catalysts: effect of metal oxides addition and SO₂, *Applied Catalysis B: Environmental* 30 (2001) 267–276
- [35] N.A. Saidina Amin, C.M. Chong, SCR of NO with C₃H₆ in the presence of excess O₂ over Cu/Ag/CeO₂-ZrO₂ catalyst, *Chemical Engineering Journal* 113 (2005) 13–25
- [36] Qingya Liu, Zhenyu Liu, Zhanggen Huang, Guoyong Xie, *Catalytic Today* 93-95 (2004) 833-837.
- [37] Brunauer. S, Emmett. P. H, Teller, E, *J. Am.Chem, Soc.* 60 309 (1938)
- [38] Rosenberg, H.S. and J. H. Oxley. “Selective Catalytic Reduction for NO_x Control at Coal-fired Power Plants” ICAC Forum’ 93, Controlling Air Toxics and NO_x Emissions, Baltimore, MD, February 24-26, 1993.
- [39] M. Schwidder, F. Heinrich, M.S. Kumar, A. Brückner, W. Grünert, *Stud. Surf. Sci. Catal.* 154 (2004) 2484.
- [40] Lisa J. Lobree, In-Chul Hwang, Jeffrey A. Reimer, and Alexis T. Bell, Investigations of the State of Fe in H-ZSM-5, *Journal of Catalysis* 186, 242–253 (1999)
- [41] Ge´rard Delahay, David Valade, Ariel Guzmá’n-Vargas¹, Bernard Coq, Selective catalytic reduction of nitric oxide with ammonia on Fe-ZSM-5 catalysts prepared by different methods, *Applied Catalysis B: Environmental* 55 (2005) 149–155
- [42] Hai-Ying Chen, Wolfgang M.H. Sachtler, Activity and durability of Fe/ZSM-5 catalysts for lean burn NO_x reduction in the presence of water vapor, *Catalysis Today* 42 (1998) 73-83
- [43] C´eline Magali Noel, Franc, oise Giulieri, Robert Combarieu, Georges Bossis, Anne Marie Chaze, Control of the orientation of nematic liquid crystal on iron surfaces: Application to the self-alignment of iron particles in anisotropic matrices, *Colloids and Surfaces A: Physicochem. Eng. Aspects* 295 (2007) 246–257
- [44] J.J. Corbett, P.S. Fischbeck and S.N. Pandis, Global nitrogen and sulfur inventories for oceangoing ships. *Journal of Geophysical Research* 104 (1999), pp. 3457–3470.
- [45] H. Choi, S.W. Ham, I.S. Nam, Y.G. Kim, *Ind. Eng. Chem. Res.* 35 (1996) 106.
- [46] P. Forzatti, *Appl. Catal. A* 222 (2001) 221.
- [47] J.L. Williams, *Catal. Today* 69 (2001) 3.

[48] M. Koebel, M. Elsener, *Ind. Eng. Chem. Res.* 37 (1998) 327.